

ISSN 1996-3343

Asian Journal of
Applied
Sciences

***In-situ* Stress Perturbation Due to Temperature Around Borehole During Carbon Injection**

Ollivia L. Sagu and William K.S. Pao

Department of Mechanical Engineering, Universiti Teknologi PETRONAS, Bandar Seri Iskandar, 31750 Tronoh, Perak, Malaysia

Corresponding Author: William K.S. Pao, Department of Mechanical Engineering, Universiti Teknologi PETRONAS, Bandar Seri Iskandar, 31750 Tronoh, Perak, Malaysia

ABSTRACT

Downhole temperature variation of CO₂ plays an important role in underground CO₂ sequestration. Along the wellbore, the temperature difference between surrounding country rock and CO₂ can cause the stress perturbation to the pre-historic *in-situ* stress, restricting the commercial injection rate and the depth of the targeted reservoir. The aim of the present study is to develop a simplified heat flow model along the wellbore, with the intention to use the generated temperature differential to study the thermal stress perturbation downhole. This study found that stress perturbation to the *in-situ* pre-historic stresses due to the temperature differential is dictated by circumferential heat transfer coefficient around the borehole, injection velocity and borehole radius. It is found that caprock is more prone to failure than the storage formation. The caprock, which has Young's modulus value twice than the sandstone, reduce the breakdown pressure by six times when subjected to the same temperature differential. *In-situ* stress anisotropy is also found to be critical to the lowering of the breakdown pressure when subjected to the same temperature differential. Under the same temperature disturbance, an increase in *in-situ* stress anisotropy lead to a lowering of the fracture initiation pressure. Both of these structural aspects put a preliminary upper limit to the maximum allowable downhole temperature variation, directly restricting the upper limit of the subsurface sequestration rate.

Key words: Thermal stress, *in-situ* stress, fracture initiation, breakdown pressure, carbon injection

INTRODUCTION

Carbon Capture and Sequestration (CCS) is one of the many ideas where excessive CO₂, particularly from power plant, can be disposed off. In CCS, CO₂ is extracted from a gas stream, pressurized and then injected into a suitable geological formation for long term storage (Lawal, 2011).

CO₂ wells are different from typical hydrocarbon wells because of large density variation of the CO₂ phasic behavior from the wellhead to the bottomhole. The transient thermal effects due to the heat loss along the injection well can decouple the surface pressure from downhole pressure (Paterson *et al.*, 2008). In other words, the observable wellhead pressure in the surface can decline while the reservoir pressure builds up and vice versa. As the stream of cold and high pressure CO₂ is injected, the temperature differential between the wellbore and the surrounding country rock will cause a stress perturbation in the injection layer. When the cold front reaches a relatively large area around the wellbore, the stress contraction produces a negative volumetric strain, which is

subsequently transmitted to the surface. One of the major concerns of CO₂ injection is the structural integrity of the formation. The stress perturbation due to the temperature differential can lower the fracture initiation pressure substantially, leading to a higher containment risk for CO₂. Theoretically, when the injectant fluid is colder than the formation temperature, the country rock surrounding the borehole will encounter a reduction in total stress (Goodarzi *et al.*, 2010). Hence, the allowable injection pressure must always be designed to take into account the lowering of fracture initiation pressure due to temperature.

The stress perturbation and structural integrity around a wellbore in a CO₂ injection scenario is a highly complex inter-disciplinary problem. It involves not only geomechanics but geo-chemical and hydrogeological processes that also influence the integrity of caprock and surrounding fault reactivation.

The objective of the present study is to formulate and investigate a simplistic breakdown stress analysis model for CO₂ injection. The model focuses on thermal stress, in particular and its effect on the *in-situ* stresses. This model is intended to be used as a 'back-of-the-envelope' tool for preliminary assessment and screening of different injection scenario.

Characteristics of CO₂: CO₂ is a colourless and odourless gas. At ambient temperature and atmospheric pressure, it is slightly heavier than air. Above its critical temperature and pressure (31°C and 74 bar), it has a similar property to a liquid which can be pumped and injected (Scharf and Clemens, 2006). Uniquely, at the supercritical condition CO₂ also has characteristic of gas. They listed characteristic of CO₂ in the underground as follows:

- Has low ability to displace formation water. After injection, it rises to the top quickly and spreads out laterally in viscous fingers or channels
- Dissolves faster but also less in water compared to oil
- On average, 50 kg of CO₂ can be dissolved in 1 m³ water under typical subsurface conditions
- May react with rock minerals, depending on the mineralogy and rock texture, formation water composition, reservoir temperature and pressure, flow rates and timing of the reaction

Storage systems: There are three formations which are used to geologically store captured carbon dioxide; depleted oil and gas reservoirs, saline aquifers, injectant for Enhanced Oil Recovery (EOR) and unmineable coalbed seams. CO₂ is injected in the supercritical state into these formations (Zahid *et al.*, 2011). In the following literature survey, the focus is on saline aquifer only.

Saline aquifer is identified as the best candidate for CO₂ storage with 1000-10000 Gt capacity. The widespread presences of saline aquifer all over the world are an added advantage. Safety concern is eliminated when it comes to offshore aquifers (Zahid *et al.*, 2011). Deep aquifers contain fossil, high salinity connate water that is not fit for industrial and agricultural use or for human consumptions. Such aquifers are already used for the injection of hazardous and non hazardous liquid waste. The high pressures encountered in deep aquifers indicate they can withstand CO₂ injection (Basbug *et al.*, 2007). Altundas *et al.* (2010) had stated that saline aquifer sequestration has no tangible benefit but by far, it has the advantage of having the largest storage potential. Thibeau *et al.* (2007) had earlier on support the motion of saline aquifer as potential and promising option for worldwide CO₂ storage capacity. There is lack of characterization experience for saline aquifers. In addition, the absence of financial incentive is not encouraging more of saline aquifer injection. Several ongoing pilot projects are In Salah in Algeria; Sleipner in Norway; Gorgon in Australia; Ketzin in Germany and US DOE Regional Parties hip Program Projects.

Risk of CCS: Garnham and Tucker (2012) had identified the 50 risks of CO₂ end-to-end injection. They had addressed the concerns of public, technical issues and stakeholder concerns into the risks. One of the major risk concerns is the safety offshore during CO₂ injection. Due to the different character of CO₂ from other hydrocarbons; heavier than air and does not require a source of ignition to be deadly, it raises questions about the possible risk it may pose.

In addition, the topside of the facilities will be exposed to very low temperatures in the event of an emergency depressurization-this will make replacement and/or protection of existing pipe work and wellheads necessary.

The low temperature of CO₂ during injection is the root of the equipment risk, geological risk and safety risks. Thus it is important to understand the temperature characteristics of carbon dioxide during injection period and the propagation of its effect.

Jimenez and Chalaturnyk (2002) had stressed on the integrity of wellbore for CO₂ injection. Wellbore is the access between the surface and the storage and is the most preferable path for leakage outside the reservoir. The integrity of a wellbore system is affected by geomechanical, geochemical and hydrogeological processes that also influence the integrity of caprock.

METHODOLOGY

The methodology of the present approach is motivated by the work of Luo and Bryant (2010). We reproduce their derivation here for the sake of completeness. We consider a differential element of fluid along the vertical distance in the well path, Δz . Energy balance of this differential element of fluid reads:

$$\frac{dH}{dz} = \frac{dQ}{dz} + g - v \frac{dv}{dz} \quad (1)$$

where, H, Q, g, v are the enthalpy per unit mass, heat loss per unit mass, gravity and average velocity of fluid, respectively. The heat loss can be described as the heat loss to the surrounding rock via the wellbore:

$$\frac{dQ}{dz} = -\frac{2\pi R h}{\dot{m}}(T - T_r) \quad (2)$$

where, R, h, \dot{m} , T_r are the wellbore radius, average value of heat transfer coefficient, injection rate and surrounding rock temperature, respectively. The surrounding rock temperature is usually a function of the vertical thermal gradient, (typical value $\sim 30^\circ\text{C}/\text{km}$) such that:

$$T_r = T_o + Gz \quad (3)$$

where, T_o is the surface temperature. The specific enthalpy is the related to the temperature differential via the heat capacity at constant pressure as:

$$dH = c_p dT \quad (4)$$

The kinetic energy term in Eq. 1 is very small compared to other term and is thus neglected. Combining Eq. 1-4 and replacing the mass flow rate with volumetric flow rate, one gets:

$$\frac{dT}{dz} = \frac{2h}{\rho c_p v R} \left(Gz + T_o + \frac{\rho v R g}{2h} - T \right) \quad (5)$$

where, $\dot{m} = \rho q = \rho v A$ and $A = \pi R^2$. If the density and heat capacity are assumed constants, Eq. 5 can be solved to obtain:

$$T = \left(T_{ow} - \frac{\alpha}{\gamma} + \frac{\beta}{\gamma^2} \right) \exp(-\gamma z) + \frac{\beta z}{\gamma} + \frac{\alpha}{\gamma} - \frac{\beta}{\gamma^2} \quad (6)$$

Where:

$$\alpha = \frac{2hT_o}{\rho c_p v R} + \frac{g}{c_p} \quad (7)$$

$$\beta = \frac{2hG}{\rho c_p v R} \quad (8)$$

$$\gamma = \frac{2h}{\rho c_p v R} \quad (9)$$

and T_{ow} is the well temperature at the surface.

Once the temperature along the well path is obtain, the bottomhole breakdown pressure, P_b , can be calculated as:

$$P_b = 3\sigma_h - \sigma_H - P_p - \Delta\sigma_T \quad (10)$$

where, σ_h , σ_H , P_p , $\Delta\sigma_T$ are the minimum *in-situ* horizontal total stress, maximum *in-situ* horizontal total stress, pore pressure and the differential thermal stress, respectively. It is tacitly assumed that the *in-situ* total vertical stress is the maximum principal stress and the horizontal *in-situ* components align with the horizontal principal directions. The thermal stress component can be calculated using the equation:

$$\Delta\sigma_T = \frac{\alpha_T E \Delta T}{1 - \nu} \quad (11)$$

where, α_T , E , ν are the thermal coefficient of expansion, Young's modulus and Poisson's ratio, respectively.

RESULTS AND DISCUSSION

To set the stage for the analysis, we assumed a vertical injection well at depth 1000 m. Material properties used for the analysis is showed in Table 1, unless otherwise stated. The main interests are the temperature variation and stress perturbation at the bottomhole where CO_2 is injected into an aquifer.

Table 1: Material properties

Parameters	Value
Well temperature (T_{wh})	15°C
Wellhead pressure (P_w)	7 MPa
Earth surface temperature (T_o)	20°C
Geothermal gradient (G)	30°C km ⁻¹
Vertical stress gradient	23 kPa m ⁻¹
Wellbore radius (R)	0.1 m
Poisson's ratio (ν)	0.3
Elastic modulus (E) (sandstone)	15 GPa
Thermoelastic coefficient (α_T)	1.5×10 ⁻⁵ 1/°K
Heat transfer coefficient (h)	22 W m ⁻²
Effective viscosity (μ)	Pa.s
Mean density of CO ₂ (ρ)	850 kg m ⁻³
Mean heat capacity of CO ₂ (C_p)	2.9 kJ kg ⁻¹ K

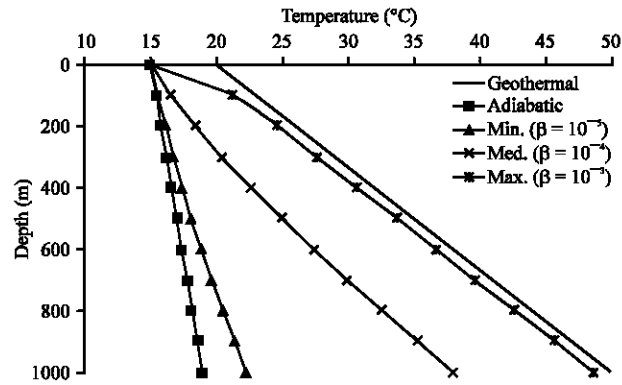


Fig. 1: Effect of β when $T_{wh} < T_o$.

Wellhead injection temperature: In the first instant, the temperature variation along the depth of injection well was investigated by assuming a lower wellhead temperature with respect to the earth surface temperature, i.e., $T_{wh} < T_o$. In this case, $T_{wh} = 15^\circ\text{C}$ was chosen with a fixed surface temperature, $T_o = 20^\circ\text{C}$. Under this circumstance, the CO₂ exists in the form of gas phase. Three different values of β with maximum, medium and minimum were assumed, each taking the value of 1×10^{-3} , 1×10^{-4} , 1×10^{-5} , respectively. Figure 1 showed the result of this analysis, together with the geothermal gradient and the adiabatic assumption plotted in Fig. 1 as reference. It is immediately clear that as the value of β becomes smaller, the CO₂ temperature along the wellbore approaches that of the adiabatic case. On the other hand, for a larger value of the CO₂ temperature gradient very quickly approaches that of the geothermal gradient except in the first hundredth meter while the CO₂ temperature remains slightly lower than its surrounding country rock. This result is consistent with the study by Luo and Bryant (2011) which showed that under normal circumstance, the CO₂ approaches the geothermal gradient at large depth.

It is also interesting to see the variation of CO₂ temperature when $T_{wh} > T_o$, which is the case shown in Fig. 2. The CO₂ at wellhead is assumed at $T_{wh} = 30^\circ\text{C}$ while the surface surrounding temperature remains the same at 20°C . In contrast to the first analysis, CO₂ under this condition exists as liquid phase. Similar trend of temperature variation is observed where for small value of

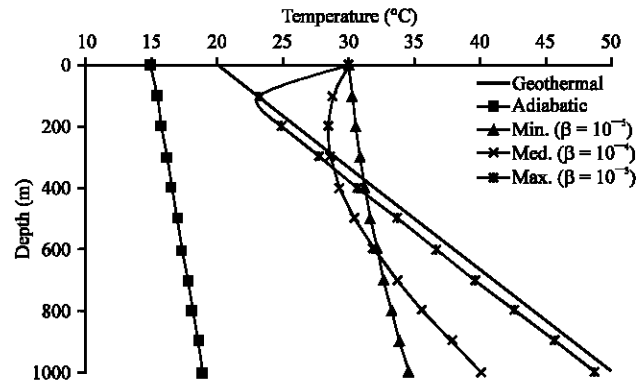


Fig. 2: Effect of β when $T_{wh} > T_o$.

β the temperature gradient of the CO_2 along the wellbore approaches that of the adiabatic case while for large value of β the CO_2 temperature gradient approaches that of the geothermal gradient. In an analytical model by Luo and Bryant (2010), they indirectly pointed out that for a situation where $T_{wh} > T_o$, the depth of intersection of CO_2 temperature gradient and the geothermal gradient is proportional to the bottomhole temperature differential. The present study confirmed their findings.

These two analyses showed that the CO_2 temperature gradient along the wellbore, on the extreme scenarios, approaches either that of the adiabatic gradient or the geothermal gradient. A further analysis of the parameter reveals that the observed characteristics of the CO_2 temperature gradient along wellbore longitudinal direction are mainly determined by three distinct factors, i.e., the wellbore circumferential heat transfer coefficient, the injection velocity and the wellbore radius, while the remaining parameters are thermodynamics properties of the injectant.

In the case where the CO_2 temperature gradient along the longitudinal direction of the wellbore approaches that of the adiabatic gradient, there is insufficient heat exchange between the CO_2 and the surrounding rock. This only happen when the circumferential heat transfer coefficient is very low (poor cement job, poor conductors etc.), the velocity of the injection is very high and the wellbore radius is so large that it prevents the radial flow of heat from happening. On the other extreme when the CO_2 temperature gradient approaches that of the geothermal gradient, the three identified parameters take on opposition characteristics, i.e., good circumferential heat transfer coefficient, low injection velocity and small wellbore radius.

Effect of injection rate: The effect of CO_2 injection rate is investigated in Fig. 3 where three injection rate of 500, 1500 and 2500 ton day⁻¹ were analyzed. It is apparent that the bottomhole temperature is inversely proportional to the injection rate. This is not surprising since at the higher flow rate, there is little time for heat loss to occur through the circumference of the wellbore. If we define the bottomhole temperature differential as $\Delta T = T_{surr} - T_{bh}$, then the temperature differential is directly proportional to the injection rate. In other words, the higher the injection rate, the more likely the increase of thermal stress according to Eq. 11.

In-situ stress perturbation: Once the CO_2 temperature profile along the longitudinal direction of the wellbore can be estimated, the bottomhole temperature is known.

Following this, the thermal stress perturbation to the *in-situ* stress can be calculated according to Eq. 10 and 11. Assuming the vertical stress gradient of 23 kPa m⁻¹ (1 psi ft⁻¹), the minimum horizontal *in-situ* stress can be estimated, theoretically, as:

$$\sigma_h = \frac{\nu}{1-\nu} \sigma_v \tag{12}$$

The solution given by Eq. 12 is usually an underestimate but for illustration purpose, we will take the theoretical value as our base case for analysis. The evaluation of the maximum *in-situ* horizontal stress, σ_H , is always problematic. Assumption is made such that the horizontal maximum *in-situ* stress to vertical stress ratio is 0.9. The pore pressure is assumed a constant gradient of 10.2 kPa m⁻¹ (0.45 psi ft⁻¹), which is of typical saline aquifer. The tensile strength of the rock is assumed as 500 kPa. Figure 4 showed that the bottomhole breakdown pressure is reduced almost by 40% for a high injection rate of 2500 ton day⁻¹. This temperature dependent lowering of the hydraulic fracture initiation pressure was identified by Hawkes *et al.* (2005) and Goodarzi *et al.* (2010).

For higher Young's modulus materials like shale, the reduction in breakdown pressure is even more pronounced as the thermal stress is directly proportional to the Young's modulus. This is

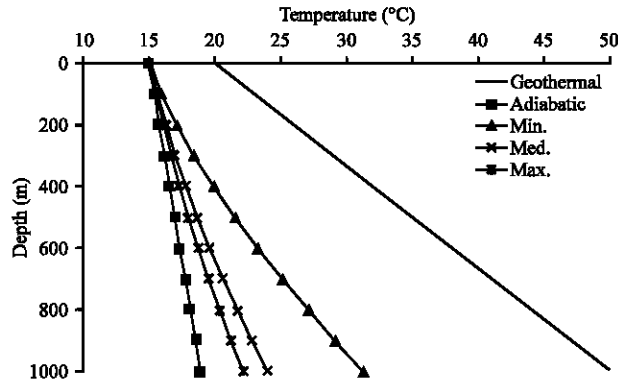


Fig. 3: Effect of injection rate (geothermal, adiabatic, minimum injection rate (500 ton day⁻¹), medium injection rate (1500 ton day⁻¹), maximum injection rate (2500 ton day⁻¹)

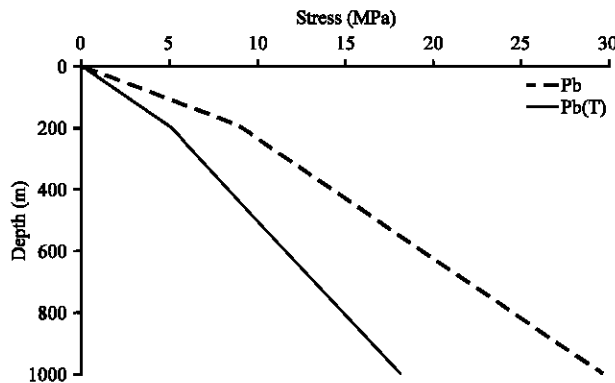


Fig. 4: Breakdown pressure with and without thermal stress

shown in Fig. 5 where the temperature effects on breakdown pressure for shale ($E = 30$ GPa) is almost three times than sandstone ($E = 15$ GPa). In other words, fine-grained clay rich materials which typically form the caprock and barrier for underground storage has a higher risk to be effected by thermal stress than the storage medium. The stiffer the material, the higher is the reduction in the breakdown pressure. Similar conclusion was reached in Goodarzi *et al.* (2010) where they showed that spontaneous fracturing is expected to take place in most CCS wells with injection temperature below reservoir temperature unless the injection rate is impractically low. However, in their paper, which utilized a very complex coupled model did not illustrate the integrity issues with respect to the caprock even though they acknowledged a more severe situation is likely to occur in the caprock in comparison to the reservoir rock. The present study, though using a simplified model, is able to give a preliminary qualitative severity of the caprock failure in comparison to the reservoir rock.

Anisotropy of *in-situ* stresses also plays an important role and should not be neglected. Figure 6 showed the effect of breakdown pressure due to horizontal stress anisotropy, in which the minimum horizontal stress gradient is assumed at 15 kPa m^{-1} . This gives a minimum horizontal to vertical stress γ_h ratio of 0.65, closer to real estimate in the field. Figure 6 showed that the higher the stress anisotropy, the lower is the breakdown pressure. This is not surprising as the higher anisotropy results in higher horizontal shear stress (if we neglected the vertical stress variation across an infinitesimal strip of rock and assumed a pancake model). Similar findings are also

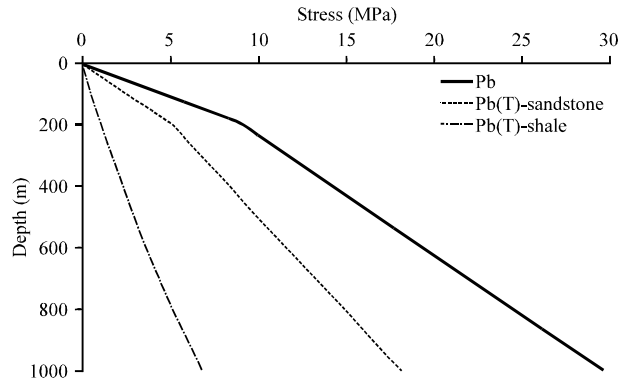


Fig. 5: Breakdown pressure for different Young's modulus

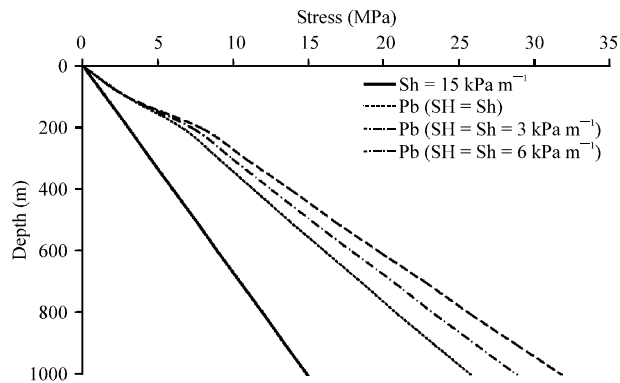


Fig. 6: Breakdown pressure due to anisotropy of *in-situ* horizontal stress

reported by Tran *et al.* (2010) in which they concluded that “High pressure in the reservoir is a necessary but not a sufficient condition to make the caprock crack. The sufficient condition depends on the magnitude of the horizontal effective stress above the caprock...” In the present study, we showed that it is not only the magnitude of the horizontal effective stress but the *in-situ* stress anisotropy.

CONCLUSION

In this study, we analyzed the effect of bottomhole stress perturbation due to the temperature differential. The analysis showed that thermal stress perturbation downhole tends to lower the breakdown pressure. The consequence of this is the lower fracture initiation pressure requirement than the isothermal analysis. We also demonstrated that caprock, which is the key containment barrier, is more prone to failure than the storage formation. Indirectly, it sets an upper limit of the possible subsurface temperature perturbation during injection. Regional geological structures with high *in-situ* pre-historic stress anisotropies are less likely to meet the storage safety requirement.

ACKNOWLEDGMENT

The author would like to acknowledge the financial support from Universiti Teknologi PETRONAS for this research under STIRF 2011/51.

REFERENCES

- Altundas, Y.B., T.S. Ramakrishnan, N. Chugunov and R. de Loubens, 2010. Retardation of CO₂ due to capillary pressure hysteresis: A new CO₂ trapping mechanism. Proceedings of the SPE International Conference on CO₂ Capture, Storage and Utilization, November 10-12, 2010, New Orleans, Louisiana, USA.
- Basbug, B., F. Gumrah and B. Oz, 2007. Simulating the effects of deep saline aquifer properties for CO₂ sequestration. *J. Can. Pet. Technol.*, 46: 30-38.
- Garnham, P. and O. Tucker, 2012. The longannet to goldeneye project: Challenges in developing an end-to-end CCS scheme. Proceedings of the Carbon Management Technology Conference, February 7-9, 2012, Orlando, FL., USA.
- Goodarzi, S., A. Settari, M. Zoback and D.W. Keith, 2010. Thermal aspects of geomechanics and induced fracturing in CO₂ injection with application to CO₂ sequestration in ohio river valley. Proceedings of the SPE International Conference on CO₂ Capture, Storage and Utilization, November 10-12, 2010, New Orleans, Louisiana, USA.
- Hawkes, C.D., P.J. McLellan and S. Bachu, 2005. Geomechanical factors affecting geological storage of CO₂ in depleted oil and gas reservoirs. *J. Can. Pet. Technol.*, 44: 52-61.
- Jimenez, J.A. and R.J. Chalaturnyk, 2002. Integrity of bounding seals for geological storage of greenhouse gases. Proceedings of the SPE/ISRM Rock Mechanics Conference, October 20-23, 2002, Irving, Texas.
- Lawal, K.A., 2011. An improved estimation of the storage capacity of potential geologic carbon sequestration sites. Proceedings of the Nigeria Annual International Conference and Exhibition, July 30 August-3, 2011, Abuja, Nigeria.
- Luo, Z. and S.L. Bryant, 2010. Influence of thermo-elastic stress on CO₂ injection induced fractures during storage. Proceedings of the SPE International Conference on CO₂ Capture, Storage and Utilization, November 10-12, 2010, New Orleans, Louisiana, USA.

- Luo, Z. and S.L. Bryant, 2011. Influence of thermo-elastic stress on fracture initiation during CO₂ injection and storage. *Energy Proc.*, 4: 3714-3721.
- Paterson, L., L. Meng, L.D. Connel and J. Ennis-King, 2008. Numerical modeling of pressure and temperature profiles including phase transitions in carbon dioxide wells. *Proceedings of the SPE Annual Technical Conference and Exhibition*, September 21-24, 2008, Denver, Colorado, USA.
- Scharf, C. and T. Clemens, 2006. CO₂ sequestration potential in austrian oil and gas fields. *Proceedings of the SPE Europec/EAGE Annual Conference and Exhibition*, June 12-15, 2006, Vienna, Austria.
- Thibeau, S., L.X. Nghiem and H. Ohkuma, 2007. A modeling study of the role of selected minerals in enhancing CO₂ mineralization during CO₂ aquifer storage. *Proceedings of the SPE Annual Technical Conference*, November 11-14, 2007, Anaheim, California, USA..
- Tran, D., K. Nghiem, V. Shrivasta and B. Kohse, 2010. Study of geomechanical effects in deep aquifer CO₂ storage. *Proceedings of the 44th U.S. Rock Mechanics Symposium and 5th U.S.-Canada Rock Mechanics Symposium*, June 27-30, 2010, Salt Lake City, UT., USA.
- Zahid, U., Y. Lim, J. Jung and C. Han, 2011. CO₂ geological storage: A review on present and future prospects. *Korean J. Chem. Eng.*, 28: 674-685.